

# QED effects in the pseudoscalar meson sector

R. Horsley<sup>a</sup>, Y. Nakamura<sup>b</sup>, H. Perlt<sup>c</sup>, D. Pleiter<sup>d</sup>,  
 P. E. L. Rakow<sup>e</sup>, G. Schierholz<sup>f</sup>, A. Schiller<sup>c</sup>, R. Stokes<sup>g</sup>,  
 H. Stüben<sup>h</sup>, R. D. Young<sup>g</sup> and J. M. Zanotti<sup>g</sup>

– QCDSF-UKQCD Collaboration –

<sup>a</sup> School of Physics and Astronomy, University of Edinburgh,  
 Edinburgh EH9 3FD, UK

<sup>b</sup> RIKEN Advanced Institute for Computational Science,  
 Kobe, Hyogo 650-0047, Japan

<sup>c</sup> Institut für Theoretische Physik, Universität Leipzig,  
 04109 Leipzig, Germany

<sup>d</sup> Jülich Supercomputer Centre, Forschungszentrum Jülich,  
 52425 Jülich, Germany,  
 Institut für Theoretische Physik, Universität Regensburg,  
 93040 Regensburg, Germany

<sup>e</sup> Theoretical Physics Division, Department of Mathematical Sciences,  
 University of Liverpool, Liverpool L69 3BX, UK

<sup>f</sup> Deutsches Elektronen-Synchrotron DESY,  
 22603 Hamburg, Germany

<sup>g</sup> CSSM, Department of Physics, University of Adelaide,  
 Adelaide SA 5005, Australia

<sup>h</sup> Regionales Rechenzentrum, Universität Hamburg,  
 20146 Hamburg, Germany

February 29, 2016

## Abstract

In this paper we present results on the pseudoscalar meson masses from a fully dynamical simulation of QCD+QED, concentrating particularly on violations of isospin symmetry. We calculate the  $\pi^+-\pi^0$  splitting and also look at other isospin violating mass differences. We have presented results for these isospin splittings in [1]. In this paper we give more details of the techniques employed, discussing in particular the question of how much of the symmetry violation is due to QCD, arising from the different masses of the  $u$  and  $d$  quarks, and how much is due to QED, arising from the different charges of the quarks. This decomposition is

not unique, it depends on the renormalisation scheme and scale. We suggest a renormalisation scheme in which Dashen's theorem for neutral mesons holds, so that the electromagnetic self-energies of the neutral mesons are zero, and discuss how the self-energies change when we transform to a scheme such as  $\overline{MS}$ , in which Dashen's theorem for neutral mesons is violated.

# 1 Introduction

Lattice calculations of the hadronic spectrum are now reaching a precision where it is essential to resolve the influence of isospin breaking effects. These have two sources, a QCD effect arising from the fact that the  $u$  and  $d$  quarks have different masses, and an electromagnetic effect due to the  $u$  and  $d$  having different electric charges. The two effects are comparable in magnitude, so a reliable calculation of isospin breaking requires simulating both the gluon and photon gauge fields.

Lattice studies of electromagnetic effects in the pions go back to [2]. In recent years the interest in QCD+QED has grown, and the pace of work accelerated [3–9].

We are carrying out simulations in QCD+QED [1]. Both gauge theories are fully dynamical, so that the electrical charges of sea-quark loops are included via the fermion determinants. We use a non-compact action for the photon field. The calculations are carried out with three clover-like quarks. Details of the lattice action will be given in section 4, and can be found in [1, 10].

In the real world, with  $\alpha_{EM} = 1/137$ , electromagnetic effects on masses are at the 1% level, or smaller. This would make them hard to measure on the lattice. Therefore we simulate with a QED coupling stronger than in real world, so that we can see effects easily, and then scale back to physical  $\alpha_{EM}$ . The simulations are carried out with  $\beta_{QED} = 0.8$ , equivalent to  $e^2 = 1.25$ ,  $\alpha_{EM} = e^2/(4\pi) \approx 0.10$ . We will see that this is a good choice, electromagnetic signals are clearly visible, much larger than our statistical errors, but we are also in a region where they still scale linearly in  $e^2$ , and we do not need to consider higher-order terms.

We generate configurations with dynamical  $u, d$  and  $s$  quarks, and then increase our data range by carrying out partially quenched calculations, with valence  $u, d, s$  quarks having different masses from the quarks used in the generation of the configurations. In addition to the  $u, d, s$  quarks, we also introduce a fictitious  $n$  quark, an extra flavour with electrical charge zero. The  $n$  quark is particularly useful for checking that we are in the region where electromagnetic effects are still linearly proportional to  $e^2$ .

In this work we present results on the pseudoscalar mesons. Our meson propagators are calculated from connected graphs only. Because we have no fermion-line disconnected graphs, the  $u\bar{u}, d\bar{d}, s\bar{s}$  and  $n\bar{n}$  states do not mix, so we can measure  $M^2(u\bar{u}), M^2(d\bar{d})$  and  $M^2(s\bar{s})$ . In the real world, these states do not exist, they mix strongly to form the  $\pi^0, \eta$  and  $\eta'$ . Disconnected graphs are responsible for the large mass of the  $\eta'$ , but will have very little effect on the mass of the  $\pi^0$ . In this work we do not consider the  $\eta$  and  $\eta'$  further, but we will need a mass for the  $\pi^0$ , with wave-function proportional to  $(u\bar{u} - d\bar{d})/\sqrt{2}$ . We

use the relation

$$M_{\pi^0}^2 \approx \frac{1}{2} [M^2(u\bar{u}) + M^2(d\bar{d})] \quad (1)$$

which is a very good approximation, with corrections proportional to the small quantity  $(m_d - m_u)^2$  [11]. This issue does not arise for the flavour non-diagonal mesons,  $\pi^+$ ,  $K^0$ ,  $K^+$ , which have no disconnected contribution.

In the first part of this paper, sections 2 to 7, we discuss theoretical questions. First we describe how our constant singlet mass procedure [11, 12] can be applied to QCD+QED. We derive a mass formula for pseudoscalar mesons in this framework. This is all that is needed to calculate physical mass splittings, in particular the  $\pi^+ - \pi^0$  splitting. It also gives us the lattice masses for the  $u, d, s$  quarks at the physical point, needed to predict mass splittings in the baryons. A particularly delicate number is the mass difference  $m_u - m_d$  (or  $m_u/m_d$  mass ratio), which is difficult to extract reliably from a pure QCD simulation, and is much better defined in QCD+QED simulations.

We also want to dissect the meson mass into a QCD part and a QED part, to find the electromagnetic  $\epsilon$  parameters, which express the electromagnetic contributions to the meson masses [13]. We find that there are theoretical subtleties in this separation, leading to scheme and scale dependence in the result.

The total energy-momentum tensor is invariant under renormalisation, and so the total mass of any hadron is independent of renormalisation scheme and scale. However the individual contributions from quarks, gluons and photons are not invariant, they all run as the energy scale increases. This is familiar in pure QCD; as the energy scale of Deep Inelastic Scattering rises, the momentum fraction carried by quarks decreases, while the momentum fraction carried by gluons increases [14]. The physical picture behind this effect is well known [15]. As  $Q^2$  rises the proton is probed with improved spatial resolution. A parton perceived as a single quark in a low- $Q^2$  measurement is resolved into multiple partons at higher  $Q^2$ , with most of the new partons being gluons.

We should expect a similar effect in QCD+QED, with improved spatial resolution revealing more photons, causing a running of energy from quarks to photons, in parallel with the running from quarks to gluons seen in QCD alone.

In QCD+QED, each hadron will be surrounded by a photon cloud. As in pure QED, the total energy in the cloud will be ultra-violet divergent. Crudely, we can think of two components of the cloud. Firstly, there are short wave-length photons, with wave-lengths small compared with a hadron radius. These can be associated with particular quarks. If we look at the hadron with some finite resolution the photons with wavelengths shorter than this resolution are incorporated into the quark masses as self energies. Secondly, there will be longer wave-lengths photons, which can't be associated with particular quarks. These photons must be thought of as the photon cloud of the hadron as a whole, these are the photons that we include when we talk of the electromagnetic contribution to the hadron mass. We expect to see many more really long wave-length photons (large compared to the hadron radius) around a charged hadron than around a neutral hadron.

Clearly, in this picture, the value we get for the electromagnetic contribution to the hadron energy is going to depend on our resolution, i.e. on the scheme and scale that we use for renormalising QED.

In the final part, section 8, we summarise our lattice results for the  $\pi^+-\pi^0$  splitting and for the scheme-dependent  $\epsilon$  parameters, which parameterise the electromagnetic part of the meson masses.

We have already published an investigation into the QCD isospin breaking arising from  $m_d - m_u$  alone in [17], and the first results of our QCD+QED program in [1], which we discuss at greater length here.

## 2 Extrapolation Strategy

In pure QCD we found that there are significant advantages in expanding about a symmetric point with  $m_u = m_d = m_s = \overline{m}$  [11, 12]. In particular, this approach simplifies the extrapolation to the physical point, and it decreases the errors due to partial quenching. We want to follow a similar approach with QED added, even though the symmetry group is smaller (the  $u$  quark is always different from the other two flavours because of its different charge).

First we find a symmetric point, with all three quark masses equal, chosen so that the average quark mass,

$$\overline{m} \equiv \frac{1}{3} (m_u + m_d + m_s) , \quad (2)$$

has its physical value. To do this, we have defined our symmetric point in terms of the masses of neutral pseudoscalar mesons

$$M^2(u\bar{u}) = M^2(d\bar{d}) = M^2(s\bar{s}) = M^2(n\bar{n}) = X_\pi^2 . \quad (3)$$

Here  $X_\pi$  is an average pseudoscalar mass, defined by

$$X_\pi^2 = \frac{1}{3} [2(M_K^\star)^2 + (M_\pi^\star)^2] \quad (4)$$

where  $\star$  denotes the real-world physical value of a mass. The  $n$  is a fictitious electrically neutral quark flavour. We have not included disconnected diagrams, so the different neutral mesons of (3) do not mix.

We also define the critical  $\kappa_q^c$  for each flavour as the place where the corresponding neutral meson is massless <sup>1</sup>

$$M^2(q\bar{q}) = 0 \quad \Leftrightarrow \quad m_q = 0 . \quad (5)$$

Chiral symmetry can be used to argue that neutral mesons are better than charged ones for defining the massless point [16].

We then make a Taylor expansion about this point, using the distance from  $\overline{m}$  as our parameter to specify the bare quark masses

$$a\delta m_q \equiv a(m_q - \overline{m}) = \frac{1}{2\kappa} - \frac{1}{2\kappa_q^{sym}} , \quad (6)$$

$$a\delta \mu_q \equiv a(\mu_q - \overline{m}) = \frac{1}{2\kappa} - \frac{1}{2\kappa_q^{sym}} , \quad (7)$$

---

<sup>1</sup>The critical  $\kappa$  defined in eq. (5) is the critical  $\kappa$  in the  $m_u + m_d + m_s = \text{const}$  surface, i.e. if  $m_u = 0$ , we must have  $m_d + m_s = 3\overline{m}$ . The  $\kappa^c$  for the chiral point with all three quarks massless will be different.

where  $m_q$  denotes the simulation quark mass (or sea quark mass), while  $\mu_q$  represents the masses of partially quenched valence quarks. Note that keeping the average quark mass constant, (2), implies the constraint

$$\delta m_u + \delta m_d + \delta m_s = 0 . \quad (8)$$

In [11] we wrote down the allowed expansion terms for pure QCD, taking flavour blindness into account. QCD+QED works very much like pure QCD. Since the charge matrix  $Q$  is a traceless  $3 \times 3$  matrix,

$$Q = \begin{pmatrix} +\frac{2}{3} & 0 & 0 \\ 0 & -\frac{1}{3} & 0 \\ 0 & 0 & -\frac{1}{3} \end{pmatrix} , \quad (9)$$

electric charge is an octet, so we can build up polynomials in both charge and mass splitting in a way completely analogous to the pure QCD case. The main difference is that we can only have even powers of the charge, so the leading QED terms are  $\sim e^2$ , while the leading QCD terms are  $\sim \delta m$ .

One very important point to note is that even when all three quarks have the same mass, we do not have full SU(3) symmetry. The different electric charge of the  $u$  quark means that it is always distinguishable from the  $d$  and  $s$  quarks.

### 3 Meson mass formula

From these considerations we find the following expansion for the mass-squared of an  $a\bar{b}$  meson, incorporating both the QCD and electromagnetic terms

$$\begin{aligned} M^2(a\bar{b}) = & M^2 + \alpha(\delta\mu_a + \delta\mu_b) + c(\delta m_u + \delta m_d + \delta m_s) \\ & + \beta_0 \frac{1}{6}(\delta m_u^2 + \delta m_d^2 + \delta m_s^2) + \beta_1(\delta\mu_a^2 + \delta\mu_b^2) + \beta_2(\delta\mu_a - \delta\mu_b)^2 \\ & + \beta_0^{EM}(e_u^2 + e_d^2 + e_s^2) + \beta_1^{EM}(e_a^2 + e_b^2) + \beta_2^{EM}(e_a - e_b)^2 \\ & + \gamma_0^{EM}(e_u^2 \delta m_u + e_d^2 \delta m_d + e_s^2 \delta m_s) + \gamma_1^{EM}(e_a^2 \delta\mu_a + e_b^2 \delta\mu_b) \\ & + \gamma_2^{EM}(e_a - e_b)^2(\delta\mu_a + \delta\mu_b) + \gamma_3^{EM}(e_a^2 - e_b^2)(\delta\mu_a - \delta\mu_b) \\ & + \gamma_4^{EM}(e_u^2 + e_d^2 + e_s^2)(\delta\mu_a + \delta\mu_b) \\ & + \gamma_5^{EM}(e_a + e_b)(e_u \delta m_u + e_d \delta m_d + e_s \delta m_s) . \end{aligned} \quad (10)$$

As well as the terms needed in the constant  $\bar{m}$  surface we have also included the term  $c(\delta m_u + \delta m_d + \delta m_s)$ , the leading term describing displacement from the constant  $\bar{m}$  surface. Including this term will be useful when we come to discuss renormalisation and scheme dependence, it could also be used to make minor adjustments in tuning.

The QCD terms have been derived in [11]. In particular, we discussed the effect of chiral logarithms in section V.C. of that paper. Briefly, since we are expanding about a point some distance away from all chiral singularities the chiral logarithms do not spoil the expansion, but they do determine the behaviour of the series for large powers of  $\delta m_q$ , (see for example equation (78) of [11]).

We will now discuss briefly the origins of the electromagnetic terms.

### 3.1 Leading order terms

In what follows we use the following notation:

$$e^2 = 1/\beta_{QED} , \quad e_q = Q_q e \quad (11)$$

where

$$Q_u = +\frac{2}{3} , \quad Q_d = Q_s = -\frac{1}{3} . \quad (12)$$

The leading order EM terms were written down in [10],

$$M_{EM}^2(ab) = \beta_0^{EM}(e_u^2 + e_d^2 + e_s^2) + \beta_1^{EM}(e_a^2 + e_b^2) + \beta_2^{EM}(e_a - e_b)^2 . \quad (13)$$

Upon examination of each of these terms in more detail, we observe that since all of our simulations have the same choice of sea quark charges, then even if we vary the sea quark masses,  $(e_u^2 + e_d^2 + e_s^2)$  is a constant, and we can simply absorb this term into  $M^2$  of (10). Hence, the  $\beta_0^{EM}$  term just stands for the fact that  $M^2$  measured in QCD+QED might be different from  $M^2$  measured in pure QCD. As we have tuned our expansion point so that the pseudoscalars have the same symmetric-point mass as in pure QCD, the  $\beta_0^{EM}$  for the pseudoscalar mesons will be zero, but we will still have to allow  $M^2$  for other particles to be different in QCD+QED than in pure QCD.

Now consider (10) at the symmetric point, for the case of a flavour-diagonal meson,  $a\bar{a}$ . At the symmetric point, nearly all terms vanish because  $\delta m_q$  and  $\delta \mu_q$  are zero. In addition, the electromagnetic terms simplify because  $e_b = e_a$ . All we are left with is

$$M^2(a\bar{a}) = M^2 + \beta_0^{EM}(e_u^2 + e_d^2 + e_s^2) + 2\beta_1^{EM}e_a^2 \quad (14)$$

at the symmetric point. However, since we have defined our symmetric point by (3), equation (14) must give the same answer whether  $e_a = -\frac{1}{3}e, 0$  or  $+\frac{2}{3}e$ , so  $\beta_1^{EM}$  must be zero (because it would split the masses of the different mesons, according to the charge of their valence quarks). However, having  $\beta_1^{EM} = 0$  for the pseudoscalar mesons does not mean that this term will also vanish for other mesons, for example the vector mesons. If we tune our masses so that the pseudoscalar  $u\bar{u}$ ,  $d\bar{d}$  and  $s\bar{s}$  all have the same mass, we would still expect to find that the vector  $u\bar{u}$  meson would have a different mass from the vector  $d\bar{d}$  and  $s\bar{s}$ , because there is no symmetry in QCD+QED which can relate the  $u$  to the other two flavours.

Finally, we observe that the contribution from  $\beta_2^{EM}$  is zero for neutral mesons,  $e_a = e_b$ . However, this is the leading term contributing to the  $\pi^+ - \pi^0$  mass splitting, so it is of considerable physical interest.

### 3.2 Next Order

Going beyond leading order, the following higher order terms of the form  $e^2\delta m_q$ ,  $e^2\delta \mu_q$  are possible:

- Sea charge times sea mass,  $\gamma_0^{EM}$

After imposing the constraints that  $\overline{m}$  is kept constant and  $e_u + e_d + e_s = 0$ , there is only one completely symmetric sea-sea polynomial left,

$$e_u^2 \delta m_u + e_d^2 \delta m_d + e_s^2 \delta m_s . \quad (15)$$

- Valence charge times sea mass

At this order all polynomials of this type are killed by the  $\overline{m} = \text{const}$  constraint.

- Valence charge times valence mass,  $\gamma_1^{EM}, \gamma_2^{EM}, \gamma_3^{EM}$

In this case there are three independent allowed terms. One convenient basis for the valence-valence terms is

$$e_a^2 \delta \mu_a + e_b^2 \delta \mu_b , \quad (e_a - e_b)^2 (\delta \mu_a + \delta \mu_b) , \quad (e_a^2 - e_b^2) (\delta \mu_a - \delta \mu_b) , \quad (16)$$

though other choices are possible.

- Sea charge times valence mass,  $\gamma_4^{EM}$

The only polynomial of this type is

$$(e_u^2 + e_d^2 + e_s^2) (\delta \mu_a + \delta \mu_b) . \quad (17)$$

Since  $(e_u^2 + e_d^2 + e_s^2)$  is held constant, this term can simply be absorbed into the parameter  $\alpha$  of (10).

- Mixed charge times sea mass,  $\gamma_5^{EM}$

At the symmetric point we can not have mixed charge terms (valence charge times sea charge), because such terms would be proportional to  $(e_u + e_d + e_s)$  which is zero. However, away from the symmetric point

$$(e_a + e_b) (e_u \delta m_u + e_d \delta m_d + e_s \delta m_s) \quad (18)$$

is allowed.

We illustrate the different physical origins of these terms by drawing examples of the Feynman diagrams contributing to each of the electromagnetic coefficients in (10), Fig. 1.

## 4 Lattice setup

We are using the action

$$S = S_G + S_A + S_F^u + S_F^d + S_F^s . \quad (19)$$

Here  $S_G$  is the tree-level Symanzik improved SU(3) gauge action, and  $S_A$  is the noncompact U(1) gauge action of the photon,

$$S_A = \frac{1}{2} \beta_{QED} \sum_{x, \mu < \nu} [A_\mu(x) + A_\nu(x + \hat{\mu}) - A_\mu(x + \hat{\nu}) - A_\nu(x)]^2 . \quad (20)$$

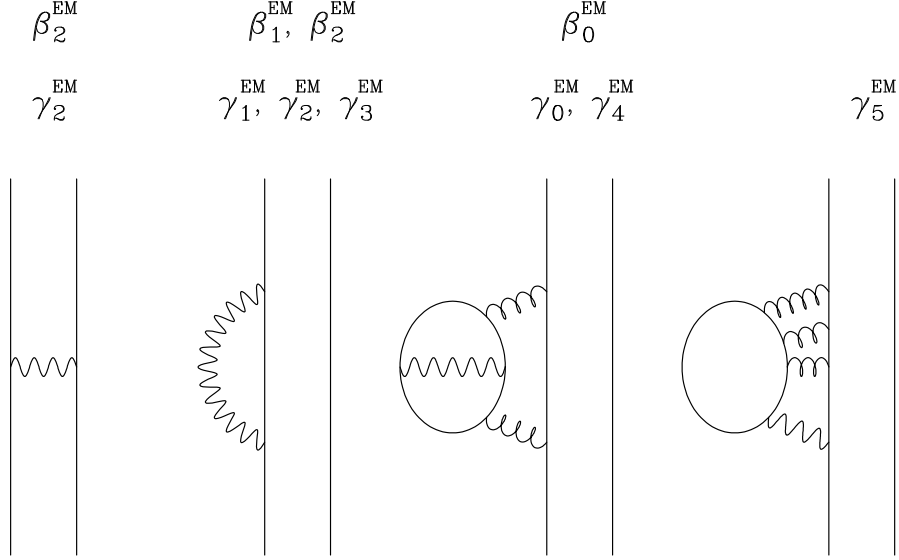


Figure 1: Examples of the Feynman diagrams contributing to each of the electromagnetic coefficients in the meson mass formula (10). All the graphs have a single photon (wavy line), and are all of  $O(e^2)$  in the electromagnetic coupling. However, some terms require multiple gluons (curly lines), and so have higher order in the strong coupling  $g^2$ .

The fermion action for flavour  $q$  is

$$\begin{aligned}
S_F^q = & \sum_x \left\{ \frac{1}{2} \sum_\mu \left[ \bar{q}(x)(\gamma_\mu - 1)e^{-iQ_q A_\mu(x)} \tilde{U}_\mu(x) q(x + \hat{\mu}) \right. \right. \\
& \left. \left. - \bar{q}(x)(\gamma_\mu + 1)e^{iQ_q A_\mu(x - \hat{\mu})} \tilde{U}_\mu^\dagger(x - \hat{\mu}) q(x - \hat{\mu}) \right] \right. \\
& \left. + \frac{1}{2\kappa_q} \bar{q}(x) q(x) - \frac{1}{4} c_{SW} \sum_{\mu, \nu} \bar{q}(x) \sigma_{\mu\nu} F_{\mu\nu}(x) q(x) \right\}, \quad (21)
\end{aligned}$$

where  $\tilde{U}_\mu$  is a singly iterated stout link. We use the clover coefficient  $c_{SW}$  with the value computed non-perturbatively in pure QCD, [18]. We do not include a clover term for the electromagnetic field. We simulate this action using the Rational Hybrid Monte Carlo (RHMC) algorithm [19].

One issue that arises in the simulation of QED is the treatment of constant electromagnetic background fields. In simulations where the electromagnetic field does not couple to the quark determinant these are electromagnetic zero modes, and so need to be handled with particular care. In this simulation the sea quarks are coupled to the electromagnetic field, and so the action does depend on the background field. However we do still need to give special treatment to these modes. We handle constant background fields by adding or subtracting multiples of  $6\pi/(eL_\mu)$  until the background field is in the range

$$-3\pi < eB_\mu L_\mu \leq 3\pi \quad (22)$$



This is the mildest way to keep the background fields under control [20]. This procedure leaves fermion determinants unchanged for particles with charges a multiple of  $e/3$ . It also leaves Polyakov loops unchanged (again, for charges in units of  $e/3$ ). We are investigating the evolution of these background fields in our simulations, and considering what effect they have on finite size effects. We plan to report on these studies in a future paper.

We have carried out simulations on three lattice volumes,  $24^3 \times 48$ ,  $32^3 \times 64$  and  $48^3 \times 96$ . The  $24^3 \times 48$  calculations show clear signs of finite size effects. The differences between  $32^3 \times 64$  and  $48^3 \times 96$  are quite small, leading us to believe that finite size effects on our largest volume are under control. In this paper we present results from the two largest volumes, which usually are in close agreement. In the few cases where there is a difference, we would favour the results from the largest volume,  $48^3 \times 96$ .

## 5 Critical $\kappa$

After several tuning runs we have been carrying out our main simulations at the point

$$\begin{aligned} \beta_{QCD} &= 5.50 , & \beta_{QED} &= 0.8 , \\ \kappa_u &= 0.124362 , & \kappa_d = \kappa_s &= 0.121713 \end{aligned} \tag{23}$$

which lies very close to the ideal symmetric point defined in (3) (but with a much stronger QED coupling than the real world,  $\alpha_{QED} = 0.099472 \dots$ , instead of the true value  $1/137$ ). At this point the  $\delta m_q$  from the sea quark masses are all zero, but we can still learn about the meson masses by varying the partially quenched valence quark masses,  $\delta \mu_q$ .

The flavour dependence of the meson masses is more complicated in QCD+QED than in pure QCD. We illustrate some of these differences in the sketch Fig. 2, showing the way that the flavour-diagonal mesons depend on the quark mass. As well as the physical charge  $+\frac{2}{3}$  and  $-\frac{1}{3}$  quarks, we also have a fictional charge 0 quark. In QCD+QED we still have the relationship  $M^2(q\bar{q}) \propto m_q$  for flavour-diagonal (neutral) mesons, but the gradients of the  $u\bar{u}$ ,  $d\bar{d}$ ,  $n\bar{n}$  mesons differ. So, in contrast to pure QCD, equal meson mass at the symmetric point no longer means equal bare quark mass. The bare mass at the symmetric point depends on the quark charge. This situation is illustrated in the left panel of Fig. 2, (though the differences between the flavours has been exaggerated for clarity).

We rescale (renormalise) the quark masses to remove this effect, making the renormalised quark masses at the symmetric point equal. The situation after renormalising in this way is illustrated in the right panel of Fig. 2. All the flavour-diagonal mesons,  $n\bar{n}$ ,  $d\bar{d}$ ,  $s\bar{s}$  and  $u\bar{u}$  now line up, depending in the same way on the new mass  $\mu^D$ , which we call the ‘‘Dashen scheme’’ mass, for reasons which should become clear later <sup>2</sup>. We will see that using this quark mass also simplifies the behaviour of the mixed flavour mesons, and helps us understand the splitting of a hadron mass into a QCD part and an electromagnetic part.

---

<sup>2</sup>Here, to introduce the idea, we just make a simple multiplicative renormalisation. In fact, the mass renormalisation matrix is not diagonal, there are also terms which mix flavours. We will include these additional terms in section 6.

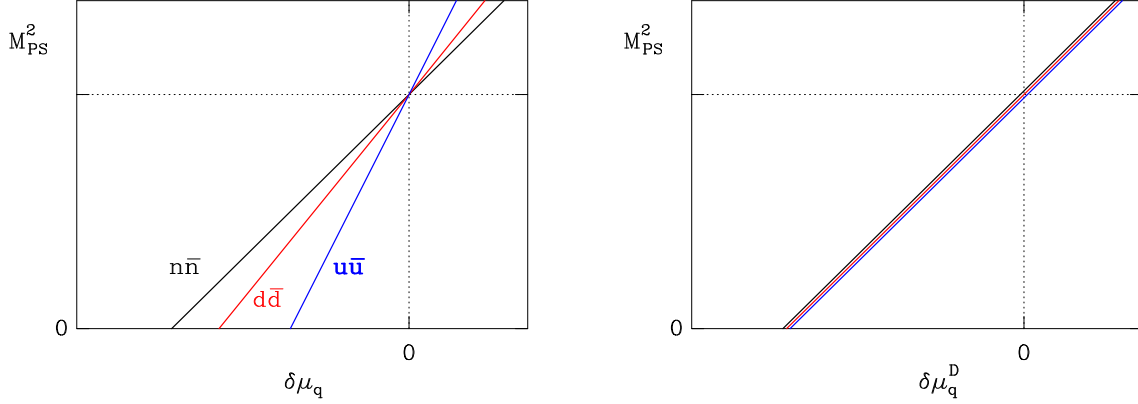


Figure 2: Sketch illustrating the transformation from bare masses (left panel) to Dashen scheme masses (right panel). In the left panel all the flavour diagonal mesons have the same mass at the symmetric point ( $\delta\mu_q = 0$ ), but have different critical points ( $M_{\text{PS}}^2 = 0$ ). In the Dashen scheme (right panel) we rescale the masses horizontally, so that all the critical points are the same. The different mesons now all depend on  $\delta\mu_q^D$  in the same way.

One way to interpret the behaviour in Fig. 2 is to consider a  $u$  and  $d$  quark with the same bare lattice mass. Since the magnitude of the charge of the  $u$  quark is twice as large as that of the  $d$  quark, it will acquire a larger self-energy due to the surrounding photon cloud and hence it will be physically more massive, which is why the mass of the  $u\bar{u}$  meson rises more steeply than the  $d\bar{d}$  meson, when plotted against bare mass. By instead plotting against the Dashen mass, we have effectively added the extra mass of the photon cloud to the quark mass. Two quarks with the same Dashen mass are physically similar in mass, and so they form mesons of the same mass, as seen in the right-hand panel of Fig. 2.

Applying these ideas to our simulations, in Fig. 3 we show how the symmetric  $\kappa^{\text{sym}}$  and critical  $\kappa^c$  are determined, using the  $d\bar{d}$  meson as an example.  $\kappa^c$  is defined from the point where the partially-quenched meson mass extrapolates to zero, (5), while  $\kappa^{\text{sym}}$  is defined by the point where the fit line crosses  $M_{\text{PS}}^2 = X_\pi^2$ , (3).

We repeat this procedure for the  $u$  and  $n$  quarks and plot the resulting  $1/\kappa^c$  and  $1/\kappa^{\text{sym}}$  values as a function of the square of the quark charges,  $Q_q^2$ , in Fig. 4 Here we clearly see that in both cases  $1/\kappa$  depends linearly on  $Q_q^2$ .

Despite appearances, the two lines are not quite parallel. In Fig. 5 we plot the bare mass at the symmetric point,

$$am_q^{\text{sym}} = \frac{1}{2\kappa_q^{\text{sym}}} - \frac{1}{2\kappa_q^c}. \quad (24)$$

$\kappa_q^c$  for each flavour is defined as the point at which the flavour-diagonal  $q\bar{q}$  meson becomes massless. We see that our data show the behaviour shown in the left-hand panel of Fig. 2, with each meson reaching the axis at a different point.

The factors needed to bring the charged bare masses into agreement with the neutral

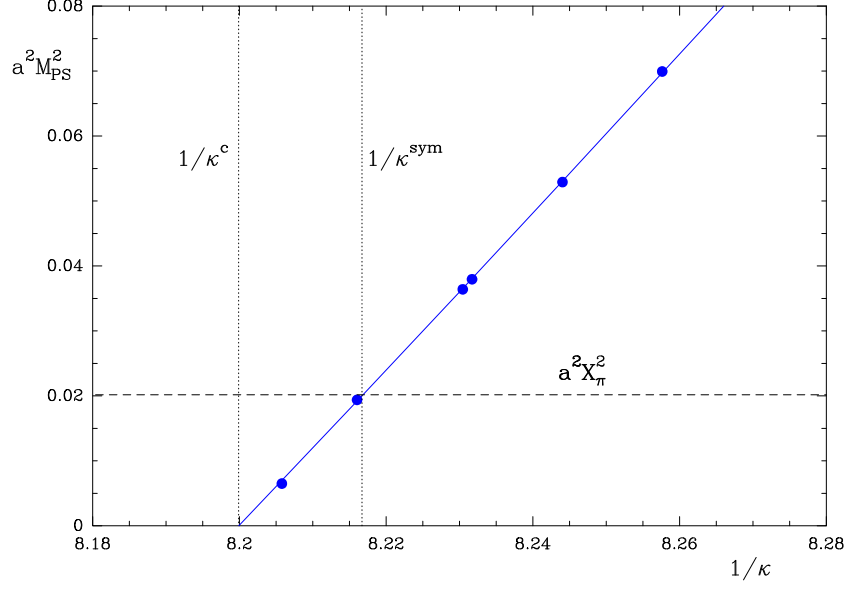


Figure 3: Determination of  $\kappa^c$  and  $\kappa^{sym}$  for the  $d$  quark.  $\kappa^c$  is defined from the point where the  $d\bar{d}$  meson mass extrapolates to zero, (5), while  $\kappa^{sym}$  is defined by the point where the fit line crosses  $M_{PS}^2 = X_\pi^2$ , (3).

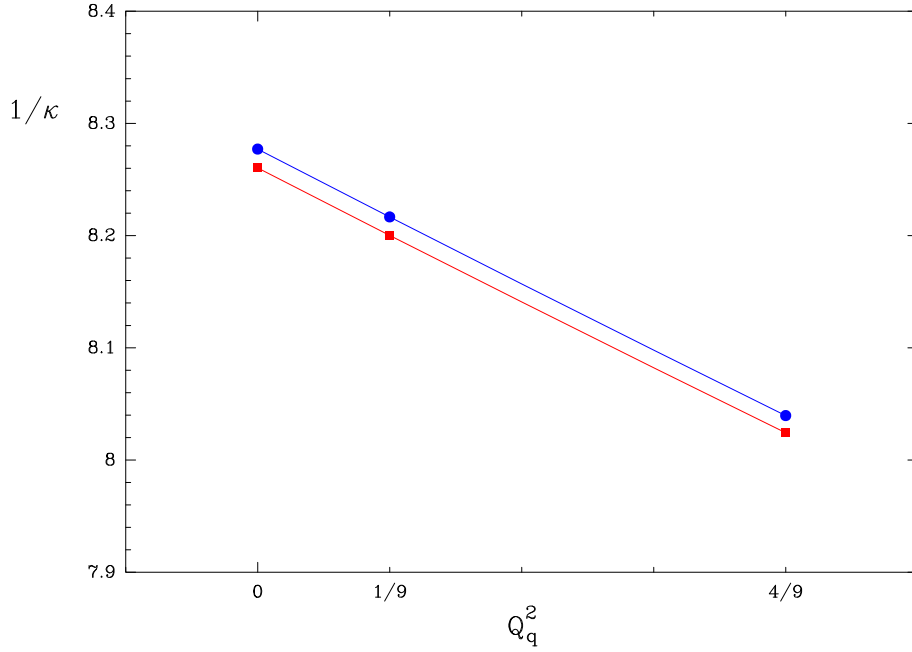


Figure 4:  $1/\kappa^c$  (red squares) and  $1/\kappa^{sym}$  (blue circles) plotted against quark charge squared,  $Q_q^2$ .

bare mass, as in the right-hand panel of Fig. 2, are

$$Z_{m_d}^{QED} = Z_{m_s}^{QED} = 1.023, \quad Z_{m_u}^{QED} = 1.096. \quad (25)$$

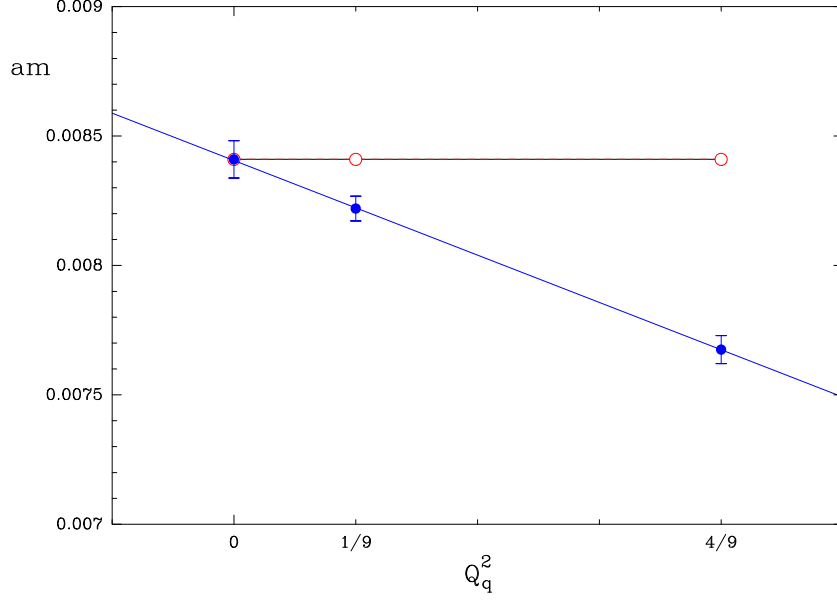


Figure 5: The bare mass at the symmetric point,  $am_q^{sym}$ , as a function of quark charge. We see that the bare mass is not constant, there is about a 10% difference between the neutral  $n$  quark and the  $u$  quark. The open red circles show the quark masses after renormalising to remove this charge dependence.

As seen in Fig. 5 this  $Z$  factor depends linearly on the quark charge squared. Hence, we can write

$$\delta\mu_q^D = (1 + Ke_q^2)\delta\mu_q = (1 + KQ_q^2e^2)\delta\mu_q, \quad (26)$$

for some constant  $K$ . By construction, this simplifies the neutral mesons as they will all lie on the same line, see Fig. 2.

In order to investigate the effect on charged mesons, we first consider the  $u\bar{u}, d\bar{d}$  and  $u\bar{d}$  ( $\pi^+$ ) meson masses plotted as a function of bare quark mass, Fig. 6. We see that in this plot the two neutral mesons,  $u\bar{u}$  and  $d\bar{d}$ , lie on different lines. We also observe that the  $\pi^+$  data do not lie on a smooth curve. This is not due to statistical errors (which are much too small to see in this plot). It is because the  $\pi^+$  meson mass depends both on  $\delta m_u + \delta m_d$ , as in pure QCD, but also has a significant dependence on  $\delta m_u - \delta m_d$ , which causes those mesons containing quarks with very unequal masses to deviate from the trend.

When we now switch to using the Dashen-scheme quark masses in Fig. 7 we see that the graph looks significantly different. The  $u\bar{u}$  and  $d\bar{d}$  mesons now lie on the same straight line (this is essentially by construction, since equal Dashen-scheme quark mass  $\Leftrightarrow$  equal neutral meson mass). More interesting is the fact that the “jiggles” in the  $\pi^+$  mass are largely removed by plotting against Dashen-scheme mass, making it much easier to estimate the EM shift in the  $\pi^+$  mass.

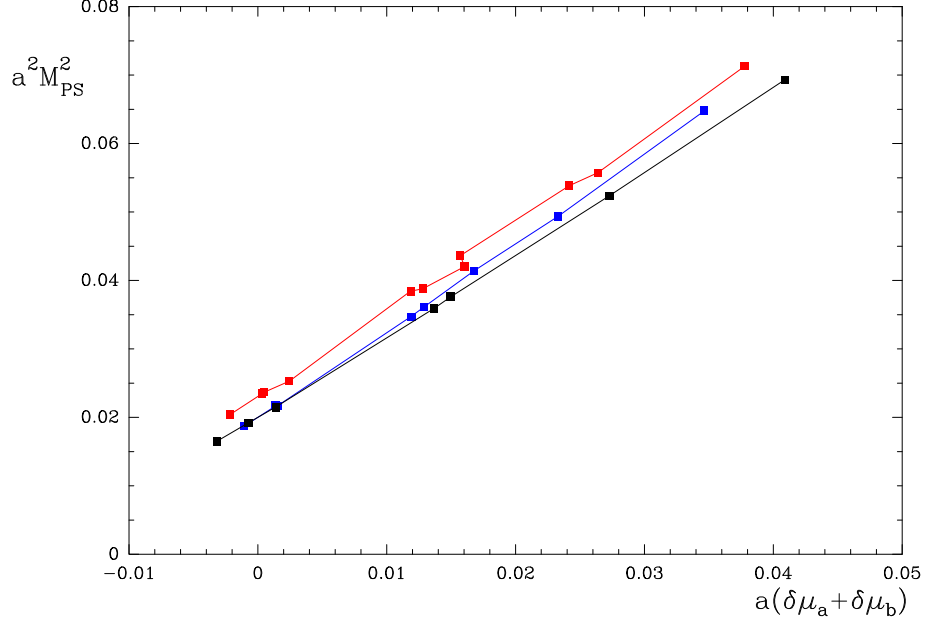


Figure 6: Pseudoscalar  $M_{PS}^2$  plotted against bare mass for the  $\pi^+$  (red),  $u\bar{u}$  (blue) and  $d\bar{d}$  (black) mesons. The lines simply connect the points. Error bars are small compared with the points. Data are from a  $32^3 \times 64$  lattice.

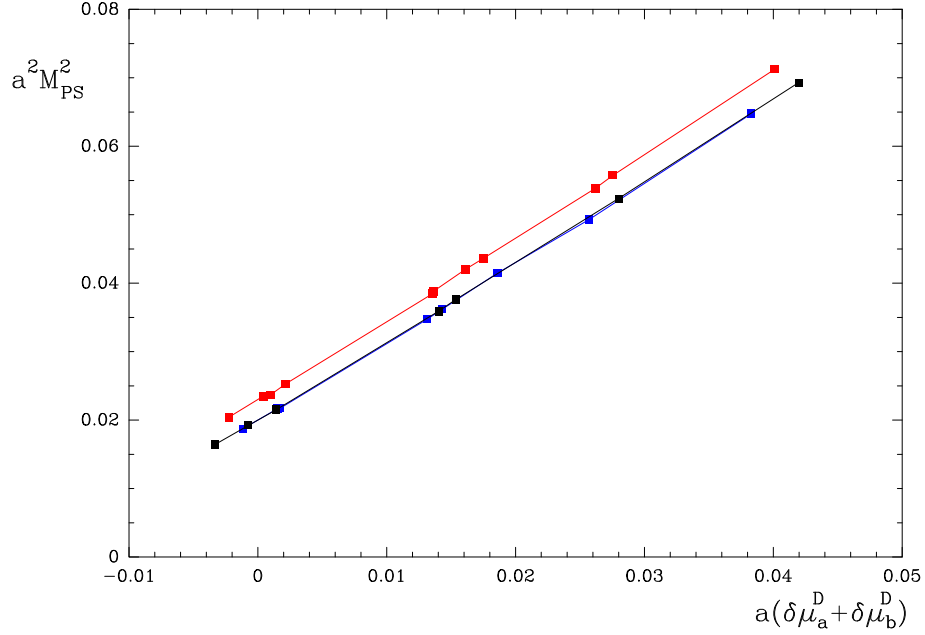


Figure 7: The same data as in Fig. 6, but this time plotted against Dashen-scheme quark mass.

## 6 Dashen scheme quark mass formula

In order to derive an expression for the meson masses in the Dashen-scheme, we start with (10) and proceed by absorbing the QED terms for the neutral pseudoscalar mesons into the quark self-energy by making the definition

$$\begin{aligned} \delta\mu_q^D &= \delta\mu_q + \left\{ \frac{1}{2}c(\delta m_u + \delta m_d + \delta m_s) + \frac{1}{2}\gamma_0^{EM}(e_u^2\delta m_u + e_d^2\delta m_d + e_s^2\delta m_s) \right. \\ &\quad \left. + \gamma_1^{EM}e_q^2\delta\mu_q + \gamma_4^{EM}(e_u^2 + e_d^2 + e_s^2)\delta\mu_q + \gamma_5^{EM}e_q(e_u\delta m_u + e_d\delta m_d + e_s\delta m_s) \right\} / \alpha. \end{aligned} \quad (27)$$

At present we are neglecting  $\gamma_0^{EM}$  and  $\gamma_5^{EM}$  because we are working on a symmetric background,  $\delta m_q = 0$ , and absorbing  $\gamma_4^{EM}$  into the coefficient  $\alpha$  because we only have data at one value of  $\beta_{QED}$ . This means that only the  $\gamma_1^{EM}$  term is used in calculating  $\delta\mu_a^D$ , giving a simple multiplicative transformation from bare mass to Dashen scheme mass. Most of the other terms in (27) represent off-diagonal terms in the quark mass  $Z$  matrix. There are many more mixing terms possible in QCD+QED than in pure QCD, but most of them first occur in diagrams with a large number of gluon and quark loops, as can be seen in Fig. 1, so they are probably rather small.

Substituting (27) into (10) we are left with the simpler formula

$$\begin{aligned} M^2(a\bar{b}) &= M^2 + \alpha(\delta\mu_a^D + \delta\mu_b^D) + \beta_0\frac{1}{6}(\delta m_u^2 + \delta m_d^2 + \delta m_s^2) \\ &\quad + \beta_1((\delta\mu_a^D)^2 + (\delta\mu_b^D)^2) + \beta_2(\delta\mu_a^D - \delta\mu_b^D)^2 + \beta_2^{EM}(e_a - e_b)^2 \\ &\quad + \gamma_2^{EM}(e_a - e_b)^2(\delta\mu_a^D + \delta\mu_b^D) + \gamma_3^{EM}(e_a^2 - e_b^2)(\delta\mu_a^D - \delta\mu_b^D). \end{aligned} \quad (28)$$

In (28) all the EM terms vanish for neutral mesons ( $e_a = e_b$ ), leaving

$$\begin{aligned} M_{neut}^2(a\bar{b}) &= M^2 + \alpha(\delta\mu_a^D + \delta\mu_b^D) + \beta_0\frac{1}{6}(\delta m_u^2 + \delta m_d^2 + \delta m_s^2) \\ &\quad + \beta_1((\delta\mu_a^D)^2 + (\delta\mu_b^D)^2) + \beta_2(\delta\mu_a^D - \delta\mu_b^D)^2, \end{aligned} \quad (29)$$

which clearly has no references to any  $EM$  coefficient, or to any charges  $e_q$ . Hence, by construction, the mass of the neutral pseudoscalar mesons comes purely from the quark masses, and has no electromagnetic contribution. The formula simplifies even further if we consider a flavour-diagonal meson

$$M^2(a\bar{a}) = M^2 + 2\alpha\delta\mu_a^D + \beta_0\frac{1}{6}(\delta m_u^2 + \delta m_d^2 + \delta m_s^2) + 2\beta_1(\delta\mu_a^D)^2. \quad (30)$$

This agrees with what we see in Figs. 2 and 7, with the different flavour-diagonal mesons all lying on the same curve when plotted against the Dashen quark mass.

In the Dashen scheme the electromagnetic contribution to the meson mass is

$$\begin{aligned} M_\gamma^2(a\bar{b}) &= \beta_2^{EM}(e_a - e_b)^2 + \gamma_2^{EM}(e_a - e_b)^2(\delta\mu_a^D + \delta\mu_b^D) \\ &\quad + \gamma_3^{EM}(e_a^2 - e_b^2)(\delta\mu_a^D - \delta\mu_b^D), \end{aligned} \quad (31)$$

while the QCD contribution is

$$\begin{aligned} M_{QCD}^2(a\bar{b}) &= M^2 + \alpha(\delta\mu_a^D + \delta\mu_b^D) + \beta_0\frac{1}{6}(\delta m_u^2 + \delta m_d^2 + \delta m_s^2) \\ &\quad + \beta_1((\delta\mu_a^D)^2 + (\delta\mu_b^D)^2) + \beta_2(\delta\mu_a^D - \delta\mu_b^D)^2. \end{aligned} \quad (32)$$

Dashen's theorems [21] state that in the limit of an exact SU(3) chiral symmetry, the neutral mesons have zero electromagnetic self energy; and that the charged mesons electromagnetic self-energies are given by a single constant. Our formulation is such as to maintain the vanishing electromagnetic self-energy of the neutral mesons away from the chiral limit. The  $\beta_2^{EM}$  term of our expansion is the generalisation of Dashens result, where, in the absence of any strong SU(3) breaking, the electromagnetic self-energy is proportional to the charge-square of the meson. The terms involving  $\gamma^{EM}$  therefore encode the deviations associated with leading-order SU(3) breaking of the strong interaction, as anticipated by Dashen.

## 7 Scheme dependence

We can calculate electromagnetic contributions to the meson masses from (31) in our scheme, but in order to compare our results with those obtained by other groups, we need to be able to quote the QED contribution in other schemes, in particular  $\overline{MS}$ .

To illustrate the issue of scheme dependence, consider the splitting between the  $K^0$  and  $K^+$  mesons. In the real world the  $K^0$ - $K^+$  splitting comes partly from QED effects, and partly from the  $m_d, m_u$  mass difference, which we consider to be the QCD part of the splitting. The ordering of the physical states, with the  $K^0$  heavier than the  $K^+$  suggests that the quark mass effect dominates, but we expect that there is still a QED contribution of comparable magnitude.

Naively, one might think that this QED contribution may be easily determined by performing a simulation with  $m_u = m_d$ . In this case, there will be no splitting from QCD, so the result will give the splitting due to QED alone. In pure QCD, setting  $m_u = m_d$  is unproblematic as equal bare mass implies equal renormalised mass, regardless of scale or scheme. However in QED+QCD, mass ratios between quarks of different charges are not invariant. The anomalous dimension of the quark mass now depends on the quark charge; at one-loop

$$\gamma_m = 6C_F g^2 + 6Q_f^2 e^2 + \dots \quad (33)$$

so the  $u$  mass runs faster than  $d$  mass. If  $m_u = m_d$  in one scheme, this will not be true in another. This also implies that there is no good way to compare masses at the physical  $e^2$  with pure QCD masses at  $e^2 = 0$ .

### 7.1 Changing Scheme

To calculate the electromagnetic part of the meson mass we take the difference between the mass calculated in the full theory, QCD+QED, ( $g^2$  and  $e^2$  both non-zero) and subtract the mass calculated in pure QCD, ( $e^2 = 0$ ):

$$M_\gamma^2 = M^2(g^2, e_\star^2, m_u^\star, m_d^\star, m_s^\star) - M^2(g^2, 0, m_u^{QCD}, m_d^{QCD}, m_s^{QCD}) . \quad (34)$$

where  $e_\star$  is the physical value of the electromagnetic coupling, corresponding to  $\alpha_{EM} = 1/137$ . In the full theory the physical quark masses are well defined: we can fix the three

physical quark masses by using three physical particle masses (the  $\pi^0$ ,  $K^0$  and  $K^+$  would be a suitable choice). In the full theory we should use the physical quark masses,  $m^*$ , but we also have to specify which quark masses we are going to use in the pure QCD case, (which is, after all, an unphysical theory). Different ways of choosing the  $m^{QCD}$  will give different values for the electromagnetic part of the meson mass.

One prescription for choosing the quark masses in the (unphysical) pure QCD case is to use the neutral meson masses. We could tune  $m^{QCD}$  by requiring

$$M_{q\bar{q}}^2(g^2, e_\star^2, m_u^*, m_d^*, m_s^*) = M_{q\bar{q}}^2(g^2, 0, m_u^{QCD}, m_d^{QCD}, m_s^{QCD}) \quad (35)$$

Since the QCD+QED mass matches the QCD mass, this scheme has zero EM contribution to neutral pseudoscalars by definition. This is our Dashen scheme, discussed above. In this scheme,  $M_\gamma^2$  is zero for neutral pseudoscalar mesons, and is given by the simple formula (31) for charged mesons.

A more conventional choice is to choose  $m^*$  and  $m^{QCD}$  the same in  $\overline{MS}$  at some particular scale. In this case, we are now presented with the task of determining the quark masses in a certain scheme (e.g. the Dashen scheme) given fixed  $\overline{MS}$  masses. Hence we need to calculate the Dashen quark masses by renormalising from  $\overline{MS}$  to the Dashen scheme:

$$\begin{aligned} m^D(g^2, e_\star^2) &= Z_m(g^2, e_\star^2, \mu^2) m^{\overline{MS}}(\mu^2), \\ m^D(g^2, 0, \mu^2) &= Z_m(g^2, 0, \mu^2) m^{\overline{MS}}(\mu^2). \end{aligned} \quad (36)$$

However, since the renormalisation factor  $Z_m$  depends on both  $g^2$  and  $e^2$ , the Dashen mass in pure QCD would not be the same as the Dashen mass in the physical QCD+QED theory:

$$m_{QCD}^D \equiv m^D(g^2, 0, \mu^2) = \frac{Z_m(g^2, 0, \mu^2)}{Z_m(g^2, e_\star^2, \mu^2)} m^D(g^2, e_\star^2) \equiv Y_m(g^2, e_\star^2, \mu^2) m^D(g^2, e_\star^2). \quad (37)$$

Hence the Dashen mass is rescaled by a renormalisation constant ratio which we denote  $Y_m$ .

Now, we know in principle what the QCD mass we should subtract is, it is the mass we get by substituting  $e^2 = 0, m^D = m_{QCD}^D$  into our fit formula. So now it is a matter of determining the ratio  $Y_m$  in (37). To proceed, we note that we already know the renormalisation factor from bare lattice mass to Dashen mass, equation (26) and (27):

$$\begin{aligned} Y_m^{latt \rightarrow D} &= 1 + \frac{\gamma_1^{EM}}{\alpha} e^2 Q_q^2 \\ &= 1 + \alpha_{EM} Q_q^2 2.20(9). \end{aligned} \quad (38)$$

We also need the renormalisation factor from bare lattice mass to  $\overline{MS}$ , which can be estimated from lattice perturbation theory [22]. Fortunately, all pure QCD diagrams with only gluons and quarks cancel because we are looking at a ratio of  $Z$  factors, so the leading contribution comes from the 1-loop photon diagram, giving

$$\begin{aligned} Y_m^{latt \rightarrow \overline{MS}} &= 1 + \frac{e^2 Q_q^2}{16\pi^2} (-6 \ln a\mu + 12.95241) \\ &= 1 + \alpha_{EM} Q_q^2 1.208. \end{aligned} \quad (39)$$



The numerical value in the second line is obtained for  $\mu = 2$  GeV and the value of the lattice spacing in our simulations,  $a^{-1} = 2.9$  GeV (see Table 2). However, the one-loop result is not the full answer, there will be higher order diagrams, with one photon plus any number of gluons, giving contributions  $\sim e^2 g^2, e^2 g^4, \dots$ . To account for these unknown terms we add an error  $\sim \pm 30\%$  to the coefficient, giving

$$Y_m^{latt \rightarrow \overline{MS}} = 1 + \alpha_{EM} Q_q^2 1.2(4) . \quad (40)$$

Combining this with (38) gives us the conversion factor from the Dashen scheme to  $\overline{MS}$  at  $\mu = 2$  GeV for our configurations ( $a^{-1} = 2.9$  GeV)

$$Y_m^{D \rightarrow \overline{MS}} = 1 - \alpha_{EM} Q_q^2 1.0(5) \equiv 1 + \alpha_{EM} Q_q^2 \Upsilon^{D \rightarrow \overline{MS}} . \quad (41)$$

We are now ready to write the transformation formula from Dashen scheme  $M_\gamma$  to  $M_\gamma$  in  $\overline{MS}$ . In the Dashen scheme

$$[M_\gamma^2]^D = M^2(g^2, e^2, [m_u^*]^D, [m_d^*]^D, [m_s^*]^D) - M^2(g^2, 0, [m_u^*]^D, [m_d^*]^D, [m_s^*]^D) \quad (42)$$

with the same Dashen-scheme quark masses in both terms. In  $\overline{MS}$

$$[M_\gamma^2]^{\overline{MS}} = M^2(g^2, e^2, [m_u^*]^D, [m_d^*]^D, [m_s^*]^D) - M^2(g^2, 0, [\tilde{m}_u]^D, [\tilde{m}_d]^D, [\tilde{m}_s]^D) \quad (43)$$

where  $[\tilde{m}_q]^D$  is given by (37)

$$[\tilde{m}_q]^D = \left(1 + \alpha_{EM} Q_q^2 \Upsilon^{D \rightarrow \overline{MS}}\right) [m_q^*]^D . \quad (44)$$

Taking the difference between (43) and (42) gives

$$[M_\gamma^2]^{\overline{MS}} - [M_\gamma^2]^D = M^2(g^2, 0, [m_u^*]^D, [m_d^*]^D, [m_s^*]^D) - M^2(g^2, 0, [\tilde{m}_u]^D, [\tilde{m}_d]^D, [\tilde{m}_s]^D) \quad (45)$$

which holds for the electromagnetic contribution to any hadron. If we are specifically interested in pseudoscalar mesons, we can use the leading order mass formula  $M^2(a\bar{b}) = \alpha(m_a + m_b)$  to give

$$\begin{aligned} [M_\gamma^2(a\bar{b})]^{\overline{MS}} &= [M_\gamma^2(a\bar{b})]^D - \alpha_{EM} \Upsilon^{D \rightarrow \overline{MS}} \alpha [Q_a^2 [m_a^*]^D + Q_b^2 [m_b^*]^D] \\ &= [M_\gamma^2(a\bar{b})]^D - \alpha_{EM} \Upsilon^{D \rightarrow \overline{MS}} \frac{1}{2} [Q_a^2 M^2(a\bar{a}) + Q_b^2 M^2(b\bar{b})] . \end{aligned} \quad (46)$$

This is a rather simple formula, the only difficulty is that at present we only have a rather rough value for the constant  $\Upsilon$ .

## 8 Lattice Results

The first question to consider is how close our simulation is to the symmetric line, where  $M(u\bar{u}) = M(d\bar{d}) = M(s\bar{s})$ . We find that at the simulation point,  $M(u\bar{u})$  is about 6% heavier than the other two mesons, so we are not quite at the desired point. In Table 1

flavour	$32^3 \times 64$	$48^3 \times 96$	simulation
$n$	0.1208142(14)	0.1208135(9)	
$d, s$	0.1217026(5)	0.1217032(3)	0.121713
$u$	0.1243838(10)	0.1243824(6)	0.124362

Table 1: The  $\kappa$  values of the symmetric point, determined from fits to the pseudoscalar meson data.

we show the  $\kappa_q^{sym}$  values determined on our two large-volume ensembles. In our fits we make a Taylor expansion about the symmetric point of Table 1, not about our simulation point. (The displacement is rather small, the difference is in the fifth significant figure.)

The next question is whether we have the value of  $\overline{m}$  correctly matched to the physical value. This is checked by comparing the averaged pseudoscalar mass squared,  $X_\pi^2$ , (4), with the corresponding baryon scale

$$X_N^2 = \frac{1}{3} [(M_N^*)^2 + (M_\Sigma^*)^2 + (M_\Xi^*)^2] . \quad (47)$$

We find  $X_N/X_\pi = 2.79(3)$ , very close to the correct physical value, 2.81, showing that our tuning has found the correct  $\overline{m}$  value very successfully.

## 8.1 The splitting of the $\pi^+$ and $\pi^0$ masses.

The first quantity we wish to consider is the mass difference between the  $\pi^+$  and  $\pi^0$  mesons. Since in this case we are calculating a physically observable mass difference there is no scheme dependence in the result.

First we need to find the  $\kappa$  values corresponding to the physical quark masses. Since we have three quark masses to determine we need three pieces of physical input, we choose the masses of the  $\pi^0$  and the two kaons

$$\begin{aligned} M_{\pi^0} &= 134.977 \text{ MeV}, \\ M_{K^0} &= 497.614 \text{ MeV}, \\ M_{K^+} &= 493.677 \text{ MeV} \end{aligned} \quad (48)$$

at  $\alpha_{EM} = 1/137$ . This determines the physical point given in Table 2. We see very close agreement between the lattice scale determined on the two lattice volumes.

Using these quark masses we now have a prediction for the one remaining meson mass, the  $\pi^+$ . Our values on the two lattice spacings are given in Table 3.

## 8.2 The $\epsilon$ parameters

The  $\pi^+-\pi^0$  mass splitting that we presented in the previous section is a physically measurable quantity, so it is independent of renormalisation. However, if we now attempt to divide our hadron masses into a QCD part and a QED part, as explained earlier, this is

	$32^3 \times 64$	$48^3 \times 96$
$a\delta m_u^*$	$-0.00834(8)$	$-0.00791(4)$
$a\delta m_d^*$	$-0.00776(7)$	$-0.00740(4)$
$a\delta m_s^*$	$0.01610(15)$	$0.01531(8)$
$a^{-1}/\text{GeV}$	$2.89(5)$	$2.91(3)$

Table 2: Bare quark mass parameters at the physical point, and inverse lattice spacing, defined from  $X_\pi$ . These masses have been tuned to reproduce the real-world  $\pi^0$ ,  $K^0$  and  $K^+$  when  $\alpha_{EM} = 1/137$ .

	$32^3 \times 64$	$48^3 \times 96$	Real World
$M_{\pi^+}$	$140.3(5)$	$139.6(2)$	$139.570$
$M_{\pi^+} - M_{\pi^0}$	$5.3(5)$	$4.6(2)$	$4.594$

Table 3: The predicted value of the  $\pi^+$  mass, and  $\pi^+-\pi^0$  splitting, in MeV.

a scheme-dependent concept. When we look with greater resolution we see more short wavelength photons, which had previously been counted as part of the quark mass, and therefore part of the QCD contribution to the mass.

The traditional way of expressing the electromagnetic contributions is through the  $\epsilon$  parameters, which measure  $M_\gamma^2$  in units of

$$\Delta_\pi \equiv M_{\pi^+}^2 - M_{\pi^0}^2, \quad (49)$$

a natural choice because it is a quantity of a similar origin, and similar order of magnitude.

The  $\epsilon$  parameters are defined by [13]

$$\begin{aligned} M_\gamma^2(\pi^0) &= M_{\pi^0}^2(g^2, e^2) - M_{\pi^0}^2(g^2, 0) = \epsilon_{\pi^0} \Delta_\pi, \\ M_\gamma^2(K^0) &= M_{K^0}^2(g^2, e^2) - M_{K^0}^2(g^2, 0) = \epsilon_{K^0} \Delta_\pi, \\ M_\gamma^2(\pi^+) &= M_{\pi^+}^2(g^2, e^2) - M_{\pi^+}^2(g^2, 0) = [1 + \epsilon_{\pi^0} - \epsilon_m] \Delta_\pi, \\ M_\gamma^2(K^+) &= M_{K^+}^2(g^2, e^2) - M_{K^+}^2(g^2, 0) = \epsilon_{K^+} \Delta_\pi = [1 + \epsilon + \epsilon_{K^0} - \epsilon_m] \Delta_\pi. \end{aligned} \quad (50)$$

$\epsilon_{K^+}$  is defined in this way so that the electromagnetic contribution to the following quantity has a simple expression

$$[M_{K^+}^2 - M_{K^0}^2 - M_{\pi^+}^2 + M_{\pi^0}^2]_\gamma = \epsilon \Delta_\pi. \quad (51)$$

From now on we will neglect the small quantity  $\epsilon_m$ , the QCD contribution to the  $\pi^+-\pi^0$  splitting, which comes largely from annihilation diagrams. This is a reasonable assumption here since we note that phenomenological estimates for the this QCD contribution are of order 0.1 MeV (or 2%) [23], which is within the precision of our present calculation.

In the Dashen scheme the  $\epsilon$  parameters are simply,

$$\epsilon_{\pi^0}^D = 0, \quad \epsilon_{K^0}^D = 0, \quad \epsilon_{\pi^+}^D = 1, \quad (52)$$

with the only non-trivial quantity,  $\epsilon^D$ , given by

$$\epsilon^D = \frac{M_\gamma^2(K^+)}{M_\gamma^2(\pi^+)} - 1 = \epsilon_{K^+}^D - 1 \quad (53)$$

On our two ensembles we find

$$\begin{aligned} \epsilon^D &= 0.38(10) & 32^3 \times 64, \\ \epsilon^D &= 0.49(5) & 48^3 \times 96, \end{aligned} \quad (54)$$

which agree within errors. In what follows, we use the  $48^3 \times 96$  value in our calculations.

Using (46) to transform these numbers into  $\overline{MS}$  with the scale  $\mu = 2$  GeV, we find:

$$\begin{aligned} \epsilon_{\pi^0} &= -\alpha_{EM} \Upsilon^{D \rightarrow \overline{MS}} \frac{1}{2} \left[ \frac{4}{9} M^2(u\bar{u}) + \frac{1}{9} M^2(d\bar{d}) \right] / \Delta_\pi = 0.03 \pm 0.02, \\ \epsilon_{\pi^+} &= \epsilon_{\pi^+}^D - \alpha_{EM} \Upsilon^{D \rightarrow \overline{MS}} \frac{1}{2} \left[ \frac{4}{9} M^2(u\bar{u}) + \frac{1}{9} M^2(d\bar{d}) \right] / \Delta_\pi = 1.03 \pm 0.02, \\ \epsilon_{K^0} &= -\alpha_{EM} \Upsilon^{D \rightarrow \overline{MS}} \frac{1}{2} \left[ \frac{1}{9} M^2(d\bar{d}) + \frac{1}{9} M^2(s\bar{s}) \right] / \Delta_\pi = 0.2 \pm 0.1, \\ \epsilon_{K^+} &= \epsilon_{K^+}^D - \alpha_{EM} \Upsilon^{D \rightarrow \overline{MS}} \frac{1}{2} \left[ \frac{4}{9} M^2(u\bar{u}) + \frac{1}{9} M^2(s\bar{s}) \right] / \Delta_\pi = 1.7 \pm 0.1, \\ \epsilon &= \epsilon^D - \alpha_{EM} \Upsilon^{D \rightarrow \overline{MS}} \frac{1}{2} \left[ \frac{4}{9} M^2(u\bar{u}) - \frac{1}{9} M^2(d\bar{d}) \right] / \Delta_\pi = 0.50 \pm 0.06. \end{aligned} \quad (55)$$

In all cases we are resolving more photons in  $\overline{MS}$ , and so converting some fraction of the quark mass into electromagnetic energy. This has very little effect in the pions because both quarks are very light, but a much larger effect in the kaons because the strange quark is heavier, and the photon cloud has a mass proportional to the quark mass.

## 9 Conclusions

We have investigated isospin breaking in the pseudoscalar meson sector from lattice calculations of QCD+QED. This allows us to look simultaneously at both sources of isospin breaking, the quark mass differences, and the electromagnetic interaction, which are of comparable importance.

The physical mass differences between the different particles are directly observable, and so must be independent of the renormalisation scheme and scale used. When we try to go beyond this, to say what fraction of a hadron's mass-squared comes from QCD, and from QED, this no longer holds — changing our resolution changes the fraction. We understand this effect, both formally, in terms of the dependence of the mass renormalisation constant on the electromagnetic coupling, and physically, in terms of the quark mass gaining a contribution from its associated photon cloud.

With this understanding, we calculate the electromagnetic contributions to hadron masses in the Dashen scheme, which is easy to implement on the lattice, and then convert these values into the more conventional  $\overline{MS}$  scheme.

We are also investigating the isospin violating mass splittings in the baryon sector [1], as well as the decomposition of these mass differences into QCD and QED parts, both in the Dashen scheme, and in  $\overline{MS}$ .

## Acknowledgements

The computation for this project has been carried out on the IBM BlueGene/Q using DIRAC 2 resources (EPCC, Edinburgh, UK), the BlueGene/P and Q at NIC (Jülich, Germany), the SGI ICE 8200 and Cray XC30 at HLRN (The North-German Supercomputer Alliance) and on the NCI National Facility in Canberra, Australia (supported by the Australian Commonwealth Government).

Configurations were generated with a new version of the BQCD lattice program [24], modified to include QCD+QED. Configurations were analysed using the Chroma software library [25].

HP was supported by DFG Grant No. SCHI 422/10-1. PELR was supported in part by the STFC under contract ST/G00062X/1, RDY was supported by the Australian Research Council Grant No. FT120100821 and DP140103067 and JMZ was supported by the Australian Research Council Grant No. FT100100005 and DP140103067. We thank all funding agencies.

## References

- [1] R. Horsley, Y. Nakamura, H. Perlt, D. Pleiter, P. E.L. Rakow, G. Schierholz, A. Schiller, R. Stokes, H. Stüben, R. D. Young and J. M. Zanotti arXiv:1508.06401 [hep-lat].
- [2] A. Duncan, E. Eichten and H. Thacker, Phys. Rev. Lett. **76** (1996) 3894 [hep-lat/9602005].
- [3] T. Blum, R. Zhou, T. Doi, M. Hayakawa, T. Izubuchi, S. Uno and N. Yamada, Phys. Rev. D **82** (2010) 094508 [arXiv:1006.1311 [hep-lat]].
- [4] S. Aoki *et al.*, Phys. Rev. D **86** (2012) 034507 [arXiv:1205.2961 [hep-lat]].
- [5] G. M. de Divitiis *et al.* [RM123 Collaboration], Phys. Rev. D **87** (2013) 11, 114505 [arXiv:1303.4896 [hep-lat]].
- [6] S. Borsanyi *et al.* [Budapest-Marseille-Wuppertal Collaboration], Phys. Rev. Lett. **111** (2013) 25, 252001 [arXiv:1306.2287 [hep-lat]].
- [7] R. Zhou *et al.* [MILC Collaboration], PoS LATTICE **2014** (2014) 024 [arXiv:1411.4115 [hep-lat]].
- [8] M. G. Endres, A. Shindler, B. C. Tiburzi and A. Walker-Loud, arXiv:1507.08916 [hep-lat].
- [9] S. Borsanyi, S. Dürer, Z. Fodor, C. Hoelbling, S. D. Katz, S. Krieg, L. Lellouch and T. Lippert *et al.*, Science **347** (2015) 1452 [arXiv:1406.4088 [hep-lat]].

- [10] R. Horsley, Y. Nakamura, D. Pleiter, P. E. L. Rakow, G. Schierholz, H. Stüben, R. D. Young and J. M. Zanotti [QCDSF Collaboration], PoS Lattice **2013** (2014) 499 [arXiv:1311.4554 [hep-lat]].
- [11] W. Bietenholz, V. Bornyakov, M. Göckeler, R. Horsley, W. G. Lockhart, Y. Nakamura, H. Perlt, D. Pleiter, P. E. L. Rakow, G. Schierholz, A. Schiller, T. Streuer, H. Stüben, F. Winter and J. M. Zanotti, [QCDSF-UKQCD Collaboration] Phys. Rev. D **84** (2011) 054509 [arXiv:1102.5300 [hep-lat]].
- [12] W. Bietenholz, V. Bornyakov, N. Cundy, M. Göckeler, R. Horsley, A. D. Kennedy, W. G. Lockhart and Y. Nakamura, H. Perlt, D. Pleiter, P. E. L. Rakow, A. Schäfer, G. Schierholz, A. Schiller, H. Stüben and J. M. Zanotti, [QCDSF-UKQCD Collaboration] Phys. Lett. B **690** (2010) 436 [arXiv:1003.1114 [hep-lat]].
- [13] S. Aoki *et al.*, Eur. Phys. J. C **74** (2014) 2890 [arXiv:1310.8555 [hep-lat]].
- [14] G. Altarelli and G. Parisi, Nucl. Phys. B **126** (1977) 298. doi:10.1016/0550-3213(77)90384-4
- [15] A. W. Thomas and W. Wiese, “The Structure of the Nucleon”, 2010.
- [16] T. Das, G. S. Guralnik, V. S. Mathur, F. E. Low and J. E. Young, Phys. Rev. Lett. **18** (1967) 759.
- [17] R. Horsley, J. Najjar, Y. Nakamura, D. Pleiter, P. E. L. Rakow, G. Schierholz and J. M. Zanotti [QCDSF-UKQCD Collaborations] Phys. Rev. D **86** (2012) 114511 [arXiv:1206.3156 [hep-lat]].
- [18] N. Cundy, M. Göckeler, R. Horsley, T. Kaltenbrunner, A. D. Kennedy, Y. Nakamura, H. Perlt, D. Pleiter, P. E. L. Rakow, A. Schäfer, G. Schierholz, A. Schiller, H. Stüben and J. M. Zanotti [QCDSF-UKQCD Collaboration] Phys. Rev. D **79** (2009) 094507 [arXiv:0901.3302 [hep-lat]].
- [19] M. A. Clark and A. D. Kennedy, Phys. Rev. Lett. **98** (2007) 051601 [hep-lat/0608015].
- [20] M. Göckeler, R. Horsley, P. E. L. Rakow, G. Schierholz and R. Sommer, Nucl. Phys. B **371** (1992) 713.
- [21] R. F. Dashen, Phys. Rev. **183** (1969) 1245.
- [22] S. Capitani, M. Göckeler, R. Horsley, H. Perlt, P. E. L. Rakow, G. Schierholz and A. Schiller, Nucl. Phys. B **593** (2001) 183 [hep-lat/0007004].
- [23] J. Gasser and H. Leutwyler, Phys. Rept. **87**, 77 (1982).
- [24] Y. Nakamura and H. Stüben, PoS Lattice **2010** (2010) 040 [arXiv:1011.0199 [hep-lat]].
- [25] R. G. Edwards and B. Joó, [SciDAC and LHPC and UKQCD Collaborations], Nucl. Phys. Proc. Suppl. **140** (2005) 832 [hep-lat/0409003].